A Comparison of Open-Source LiDAR Filtering Algorithms in a Mediterranean Forest Environment

Antonio Luis Montealegre, María Teresa Lamelas, and Juan de la Riva

Abstract—Light detection and ranging (LiDAR) is an emerging remote-sensing technology with potential to assist in mapping, monitoring, and assessment of forest resources. Despite a growing body of peer-reviewed literature documenting the filtering methods of LiDAR data, there seems to be little information about qualitative and quantitative assessment of filtering methods to select the most appropriate to create digital elevation models with the final objective of normalizing the point cloud in forestry applications. Furthermore, most algorithms are proprietary and have high purchase costs, while a few are openly available and supported by published results. This paper compares the accuracy of seven discrete return LiDAR filtering methods, implemented in nonproprietary tools and software in classification of the point clouds provided by the Spanish National Plan for Aerial Orthophotography (PNOA). Two test sites in moderate to steep slopes and various land cover types were selected. The classification accuracy of each algorithm was assessed using 424 points classified by hand and located in different terrain slopes, cover types, point cloud densities, and scan angles. MCC filter presented the best overall performance with an 83.3% of success rate and a Kappa index of 0.67. Compared to other filters, MCC and LAStools balanced quite well the error rates. Sprouted scrub with abandoned logs, stumps, and woody debris and terrain slopes over 15° were the most problematic cover types in filtering. However, the influence of point density and scan-angle variables in filtering is lower, as morphological methods are less sensitive to them.

Index Terms—Airborne laser scanning, ground filtering algorithms, Mediterranean forest, open-source software.

I. INTRODUCTION

AIRBORNE light detection and ranging (LiDAR) has gradually become a common tool for collecting elevation information of surface targets with high precision and great density by calculating the time of flight taken for laser pulse travel between the LiDAR sensor and the target [1], [2]. Compared to the traditional photogrammetric method, the accuracies of the LiDAR measurements, approximately 0.15 m in altimetry and 1 m in planimetry under best conditions [3],

are unaffected by external light conditions, and its high spatial resolution outperforms the use of synthetic aperture radar (SAR) [4]. Furthermore, by distinguishing between the different reflections of a laser pulse, airborne LiDAR systems are capable of penetrating through vegetation, and recording the terrain beneath it [5]. Therefore, LiDAR has been widely used in digital elevation models (DEMs) generation, essential in environmental surveying and planning applications [6]. Since the raw LiDAR data contain a large number of points returned from various surface objects, such as buildings, bridges, electrical wires, and trees, these nonground/object points should be separated, the so-called LiDAR data filtering, prior to DEM construction. Conversely, bare-earth points need to be removed to accurately identify nonground objects [7].

According to several studies, the accuracy of a DEM developed with LiDAR data depends on: 1) the sensor and flight parameters, i.e., operating principles, scanner device, flight altitude, and speed [8], [9]; 2) the Earth's surface characteristics, i.e., topography and land cover [10]; and 3) the processing techniques used to create the DEM, i.e., filtering and interpolation methods, resolution, etc. [11]–[14]. However, Fisher and Tate [15] argue that relatively few studies have investigated error propagation between stages in DEM development. For instance, nonground points classified as ground, i.e., Type II or commission errors, may result in erroneous surface morphologies. Similarly, Type I or omission errors may lead to sparse ground points, failing to depict surface morphology [16].

On the other hand, a significant body of research has focused on LiDAR point classification, resulting in the development of several filtering methods, such as interpolation-based [5], [17]–[19], slope-based [20]–[22], segmentation-based [23], and morphological ones [24]–[26]. Meng *et al.* [27] identify some key assumptions in which most algorithms are based: 1) most of the terrain surfaces are locally autocorrelated and continuous, and the ground and nonground points exhibit an abrupt change in elevation; 2) as the terrain surface may be occluded, for instance by vegetation, the size of the local neighborhood should be adjusted to ensure that the terrain points are included; 3) the sizes of objects are within a limited range; 4) the lowest LiDAR points in a defined neighborhood have a higher probability of belonging to the terrain. Current approaches usually use these concepts independently or integrate several of them [28].

Filtering algorithms are typically tested using computer-simulated datasets for which the true ground is known [25]. In order to avoid the use of particular datasets and facilitate a meaningful comparison of performance between algorithms, Sithole and Vosselman [29] validated the performances of eight

classical filtering methods, in eight reference study sites (four urban and four rural), based on 15 samples representative of different environments, provided by the International Society for Photogrammetry and Remote Sensing (ISPRS) commission. They concluded that most filters perform well in flat and non-complex sceneries, but present problems in steep landscapes of dense vegetation. The last may be due to one of the assumptions of filtering algorithms: the bare-earth surface is smoother than the object's surface [14], [27]. Consequently, optimizing the algorithm parameters in large and topographically complex areas is still required [14], [18], [30]. Zhang and Whitman [30] pointed out the better performance of surface-based filters as more context information is used in the filtering process than in other strategies [31]. One of these methods presented by Axelsson [32] obtained better results in terms of total error in almost all reference study sites. From 2004 onward, several new filtering methods [26], [33]–[36] have been developed and evaluated based on the ISPRS dataset [37]. However, these methods perform even worse than that of Axelsson [32]. In addition, many reported results (e.g., [18] and [36]) correspond to researches applied to data with relatively high point densities and collected from low flight heights, typically 200–300 m above ground. In this sense, the need of filtering assessment arises when LiDAR datasets present medium–low nominal point density, as it is the case of the LiDAR data provided by the Spanish National Plan for Aerial Orthophotography (PNOA) with 0.5 points/m^2.

Most filtering methods offer a strong theoretical background, but they are still application specific, as they require additional information about the studied area to achieve satisfactory results. For example, knowledge-based methods, specially developed for characterizing cityscapes, have been exploited to include terrain information [38], [39] but extensive databases, sometimes difficult to obtain, are required [40]. Recently, statistically based methods have been introduced [36], [40]–[42] to achieve parameter-free methods based on skewness balancing. However, a set of conditions needs to be satisfied, e.g., a minimum number of ground points to be used [40]. Consequently, they are unable to remove attached objects and preserve ground points with irregular height distribution [36].

Despite the development of new methods and the widespread use of LiDAR-derived DEMs, filtering has been proven to be exceptionally difficult to automate especially in applications with large datasets in areas of diverse terrain characteristics [33], [36], [43]. Furthermore, there is little guidance in the literature regarding the selection of parameters, e.g., thresholds and window sizes, to be included to optimize filtering [6], [19], [30]. In fact, point classification algorithms commonly applied by LiDAR vendors are proprietary knowledge, being very often gray- or black-box approaches, not readily available for independent validation and comparison. Fortunately, in recent years open-source algorithms designed for discrete-return LiDAR data have been developed, which can be independently tested, evaluated, and compared [44], [45].

Due to the lack of an optimal filtering algorithm, a quality control becomes necessary to select the most suitable in a particular context. The influence of different variables like pulse density, terrain slope, and vegetation on the vertical accuracy

of LiDAR-derived DEMs has been commonly assessed [12]; however, little research has focused on the comparison of different point classification algorithms. Therefore, the research objectives of this paper are: 1) to evaluate the relative performance of seven different well-known filtering methods available in nonproprietary software, the progressive TIN densification algorithm (LAStools), the weighted linear least-squares interpolation-based method (FUSION), the multiscale curvature classification (MCC), the interpolation-based filter (BCAL), the elevation threshold with expand window method (ETEW-ALDPAT), the progressive morphological filter (PM-ALDPAT), and the maximum local slope algorithm (MLS-ALDPAT), in medium–low density point clouds captured in a forest environment; 2) to determine the influence of terrain slope, land cover, point density, and scan angle in the filtering error; and 3) to provide guidance for users of PNOA LiDAR point clouds to select the most suitable filtering algorithm to be applied in a Mediterranean pine forest using nonproprietary tools.

II. MATERIAL AND METHODS

A. Study Area

The study area consists of two sample sites, T1 (2 km × 2 km) and T2 (4 km × 2 km), located in the central Ebro valley (41° 56′ N, 0° 56′ W), sited northeastern Spain (Fig. 1). The Ebro Basin constitutes the northernmost semi-arid region in Europe and stretches from the Pyrenees range, in the north, to the Iberian range, in the south.

This area presents a Mediterranean climate with continental features. Annual precipitation is low, averaging 350 mm, and presents an irregular distribution during the year, mostly concentrating in autumn and spring. Moreover, the study area is characterized by cold winters, with monthly mean temperature about 7 °C, and hot, dry summers, with temperatures about 24 °C [46]. With respect to topography, the area presents a hilly relief, with elevation ranging from 400 to 750 m above sea level, and moderate-to-steep slopes (Fig. 2).

In the two selected sites, Aleppo pine forests (*Pinus halepensis* Mill.) cover 528 ha and pine terrace plantation 30 ha, being interspersed with evergreen shrubs, dominated by *Quercus coccifera* L., *Juniperus oxycedrus* L. subsp. *macrocarpa* (Sibth. & Sm.) Ball and *Thymus vulgaris* L. covering a total of 302 ha, and cereal crops account for 115 ha (see Table I).

The forest presents a homogeneous structure, an average canopy height of 6.5 m and an average biomass of 45 t/ha. Old stands reach 12–13 m in height and 90 t/ha of biomass [47]. In addition, in the last century, the study site has been recurrently affected by fire, some areas being burned even twice. Two scars of wildfires developed in June 1995 and August 2008, which consumed 5300 ha of forest, are distinguishable nowadays [48]. Particularly, the west end of T2 is covered by 232 ha of coniferous forest affected by a wildfire in 2008. Currently, the vegetation of this area is dominated by shrub species that colonize rapidly, while the succession to forest needs considerably longer time [49]. Thus, this study area is characteristic of a Mediterranean environment, repeatedly affected by wildfires
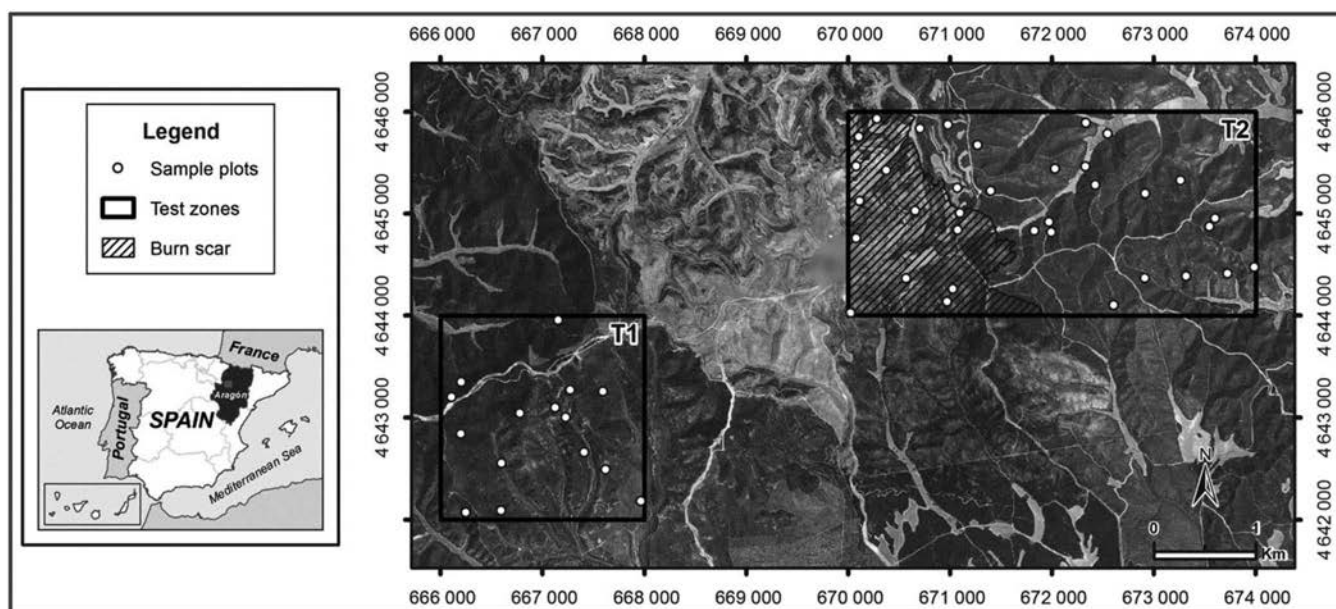
Fig. 1. Study area (T1 and T2 sites) and the 50 random sample plots. As background a high spatial resolution orthophotography (source: PNOA 2009).
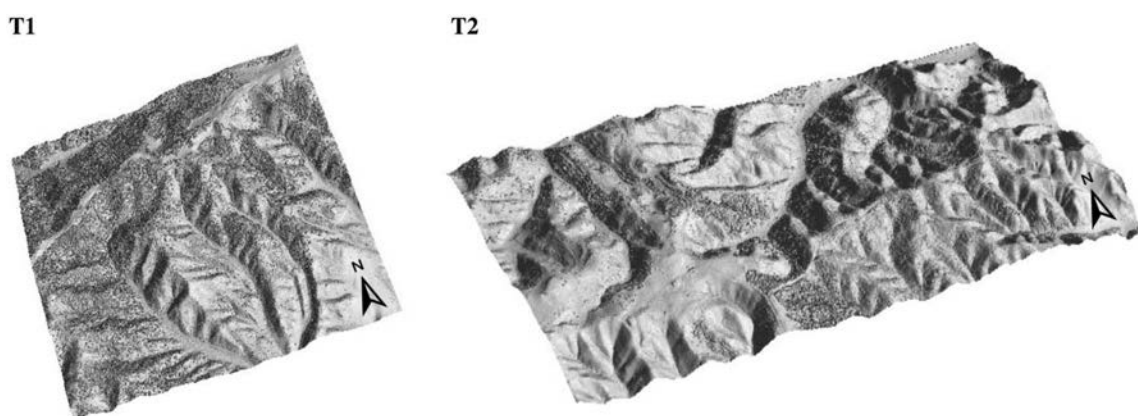

Fig. 2. 3-D shaded surface models from unfiltered LiDAR PNOA point clouds of test sites: T1 and T2.

TABLE I
SUMMARY OF TEST SITES T1 AND T2 CHARACTERISTICS

Test site	Mean elevation (m)	Elevation range (m)	Mean slope (degrees)	Slope range (degrees)	Coniferous forest (%)	Pine terrace plantation (%)	Shrub (%)	Crops and grasslands (%)	Burned area (%)
T1	661	162	16	38	27	8	51	14	0
T2	627	262	16	41	52	0	12	7	29

[50]. As a result, the landscape is a patchwork of bare ground, fields, shrubs, tree skeletons, and stands of coniferous forest.

B. LiDAR Data Acquisition

The LiDAR data were provided by the PNOA (http://www.ign.es/PNOA/vuelo_lidar.html) and captured in several surveys conducted between January 22 and February 5, 2011, using an airborne Leica ALS60 discrete return sensor. Data were delivered in three $2\,\text{km} \times 2\,\text{km}$ tiles of raw data points in LAS binary file, format v. 1.1, containing x- and y-coordinates (UTM Zone 30 ETRS 1989), ellipsoidal elevation z (ETRS

1989), with up to four returns measured per pulse and intensity values from a 1064-nm wavelength laser. The resulting LiDAR point density of test areas was $1\,\text{point}/\text{m}^2$ with a vertical accuracy higher than 0.20 m. The properties of the LiDAR acquisition are summarized in Table II. It should be noted that all returns were used in the processing.

C. Software and Ground Filtering Algorithms Evaluated

The filters used to separate ground and nonground point measurements in the selected test areas include: progressive TIN densification (LAStools), weighted linear least squares

TABLE II
LiDAR Data Specifications and Acquisition Properties

Property	Value
Sensor	ALS60
Scanning method	Oscillating plane mirror (saw-tooth pattern)
Date	January and February 2011
Mean flying height above ground (m)	3012
Mean flying speed (km/h)	241
Laser return density (point/m^2)	1.0
Field of view (degrees)	40
Beam divergence angle (mrad)	0.22
Scan angle (degrees)	±22°
Total extension of LAS files (km^2)	12
Point count	18 495 618
Altimetric accuracy (RMSE in m)	0.20

interpolation-based (FUSION), multiscale curvature classification (MCC), interpolation-based (BCAL), elevation threshold with expand window (ETEW), progressive morphological (PM), and maximum local slope (MLS). All filters are surface-based methods, as the core step of this kind of methods is to create a parametric surface approximating the bare earth with a buffer zone that defines a region in three-dimensional (3-D) space where ground points are expected to reside [29]. Depending on the way of creating the surface, these methods can be further divided into interpolation-based, progressive TIN densification, and morphology-based subcategories [31]. An overview of the software and a characterization of the filters associated with them is given in Table III and described below in more detail.

1) LAStools: LAStools is a suite of LiDAR data-processing tools programmed by Martin Isenburg. The tool *lasground* was used to label each point as ground point or not (http://rapidlasso.com/lastools/). This tool implements the method proposed by Axelsson [32], [51], which is based on a grid simplification. First, this algorithm divides the whole-point dataset into tiles and selects the lowest points in each tile as the initial ground points. Then, a triangular irregular network (TIN) of those ground points is constructed as the reference surface. In each triangle of the TIN, one of the unclassified points is added to the set of ground points following two criteria: the point's distance to the TIN facet and the angle between the TIN facet and the line connecting the point with the closest vertex of the facet must not exceed a given thresholds. Before the next iteration, all ground points classified in the current iteration are added to the TIN. In this way, the triangulation is progressively densified until all points are classified as either ground or object [6], [31]. In practice, parameterization of *lasground* consists of the selection of two settings: the terrain type (a step size of 5 m, suitable for forest and mountains, was selected) and the granularity, i.e., how much computational effort to invest into finding the initial ground estimate (the options "default" and "fine" were selected).

2) FUSION: FUSION v. 3.30 software [52] was developed at the U.S. Forest Service Pacific Northwest Research Station (http://forsys.cfr.washington.edu/fusion/fusionlatest.html). The command *groundfilter* used to generate a bare-earth surface is adapted from Kraus and Pfeifer [5] and is based on linear prediction [53], which belongs to the category of so-called interpolation-based filters. These type of filters usually fit a surface to the data and iteratively classify points based on a function to assign weights to each point (pi) based on its residual (vi) from the fitted surface. In the first iteration, all points are given equal weights and an averaging surface model is computed, so the residuals of the data points relative to the surface are calculated [54]. If the measured points lie above it, they have less influence on the shape of the surface in the next iteration, and vice versa [5], i.e., ground points are more likely to have negative residuals, so they are given more weight in subsequent iterations and thus they attract the computed surface toward themselves [6], [31], [54]. The g*roundfilter* command computes the weights for each LiDAR point using (1)

$$p_i = \begin{cases} 1 & v_i \le g \\ \frac{1}{1+(a(v_i-g)^b)} & g < v_i \le g + w \\ 0 & g + w < v_i \end{cases} . \qquad (1)$$

The parameters a and b determine the steepness of the weight function. The FUSION manual recommends values of 1.0 and 4.0 for a and b, respectively, in most applications. The shift value g determines which points are assigned a maximum weight of 1.0. Points located a higher distance than g below the surface are assigned a weight of 1.0. The above-ground offset parameter w is used to establish an upper limit to points having an influence on the intermediate surface. Points above the level defined by $(g + w)$ are assigned a weight of 0.0. In the current implementation, values for g and w are fixed throughout the filtering run. Kraus and Pfeifer [5] used an adaptive process to modify the g parameter for each iteration. After the final iteration, default is 5, ground points are selected using the final intermediate surface. All points with elevations that satisfy the first two conditions of the weight function are considered bare-earth points [52]. In the absence of guidance to select appropriate values and given the numerous possible combinations, experimentation by setting different parameter values was performed.

3) Multiscale Curvature Classification: MCC-LiDAR v.2.1 is an open-source command-line tool developed to process discrete-return LiDAR data in forest environments and is available on http://sourceforge.net/p/mcclidar/wiki/Home/. It classifies data points as ground or nonground using the MCC algorithm, developed by Evans and Hudak [19] at the Moscow Forestry Sciences Laboratory of the USFS Rocky Mountain Research Station.

Like FUSION 3.30 software [52], MCC is an iterative-interpolation-based filter. The MCC algorithm operates by discarding returns that exceed a threshold curvature, calculated from a surface interpolated using a thin-plated spline. Through three successively larger scale domains that define the processing window size, the algorithm iterates until the number of remaining returns changes by less than 1%, less than 0.1%, and

TABLE III
EVALUATED FILTERING ALGORITHMS AND KEY PARAMETERS

Software/tool	Developer	Filter description	Key parameters
LAStools—"*lasground.exe*"	Martin Isenburg adapted from Axelsson [32], [51]	Progressive TIN densification	Terrain type, granularity
FUSION—"*groundfilter.exe*"	Robert J. McGaughey adapted from Kraus and Pfeifer [5]	Interpolation-based	Weight assigned to points (*g, w, a, b* parameters), cell size
MCC—LiDAR	Evans and Hudak [19]	Interpolation-based	Scale, curvature
BCAL LiDAR Tools—"*Perform Height Filtering*"	Streutker and Glenn [55]	Interpolation-based	Return number, canopy spacing, threshold value, interpolation method, maximum iteration
ALDPAT—"*Elevation Threshold with Expand Window (ETEW) filter*"	Zhang and Whitman [30]	Morphology-based	Initial cell size, slope factor, number of iteration
ALDPAT—"*Progressive Morphological (PM) filter*"	Zhang *et al.* [25]	Morphology-based	Initial cell size, window size, slope, initial threshold
ALDPAT—"*Maximum Local Slope (MLS) filter*"	Vosselman [20]	Morphology-based	Cell size, search radius, slope threshold

finally less than 0.01% in the three scale domains, respectively [19], [44].

There are two parameters that must be defined in the command-line syntax to run MCC: the scale parameter (s) and the curvature threshold (t). The optimal scale parameter is a function of the scale or size of the objects and point spacing of the LiDAR data. Since the point spacing of the test areas is 1 m, a scale parameter of 1 was determined and three values were tested for the curvature threshold, 0.3, 0.4, and 0.5 as recommended by the developers of this algorithm.

4) BCAL LiDAR Tools: BCAL LiDAR Tools v.1.5.1 was originally developed by David Streutker from the BCAL of Idaho State University and is distributed through http://bcal. boisestate.edu/tools/lidar/. BCAL LiDAR Tools have also been used by ITT Exelis to develop their own proprietary LiDAR extension for ENVI software. The *Perform Height Filtering* tool designed for optimal performance in shrub–steppe ecosystems [55] classifies LiDAR data into ground and vegetation. It is a grid-based classification algorithm that first identifies the lowest elevation point in a search area determined by the user, and then creates a surface by interpolating these lowest points [55]. This tool uses several interpolation methods, such as cubic spline, inverse distance, inverse multicuadric, linear, natural and nearest neighbor, polynomial regression, and thin plate spline. In subsequent iterations, any point that lies on or below the previous iteration's surface is classified as ground and is included in subsequent iterations until no unclassified returns remain below the interpolated surface. Then, all unclassified returns above the surface are classified as object [55].

5) Airborne LiDAR Data Processing and Analysis Tools: ALDPAT v.1.0 was developed by the National Center for Airborne Laser Mapping (NCALM). This software implements several algorithms to classify the ground and nonground LiDAR measurements [56] and is available on http://lidar. ihrc.fiu.edu/index.html. This group of morphology-based filters derived from mathematical morphology [57] is based on the combination of two basic operations, the so-called closing (erosion after dilation) and opening (dilation after erosion), to

determine the minimum and maximum points within a certain structure element (window) and to remove the object returns [6], [24]. The collection of algorithms used is described below.

a) ETEW filter: This filter is based on the Zhang and Whitman [30] algorithm. The LiDAR dataset is subdivided into an array of square cells and all points, except the minimum elevation, are discarded. In the next iteration, the cells are increased in size and the minimum elevation in each cell is determined. Then, all points with elevation higher than a threshold above the minimum are discarded. This process is repeated for increasing cells and thresholds in size until no points from the previous iteration are discarded [30], [56].

b) PM filter: Zhang *et al.* [25] developed a PM filter to differentiate between ground and nonground points based on elevation differences between cells in a moving window using morphological operations such as openings and closings. The PM filter removes the measurements in different sized nonground objects, while preserving ground data to derive a parametric surface model, by gradually increasing the window size and using elevation thresholds. The process ends when the size of the filtering window is larger than the predefined maximum size of nonground objects. The cell size is usually selected to be smaller than the average spacing between LiDAR measurements to preserve the highest amount of points. If no measurement exists in a cell, the value of its nearest neighbor is assigned.

c) MLS filter: Vosselman [20] developed a filter that describes the maximum admissible height difference within a structure element (circular window) as a function of the distance calculated as the horizontal euclidean distance between two points, the so-called local slope concept. Since terrain slope is usually different from the slope observed between the ground and the tops of trees, this slope or gradient difference can be used to separate ground and nonground measurements from a LiDAR dataset. Each point measurement from the cloud is assigned into a cell of an array in terms of its x- and y-coordinates. If more than one point falls in the same cell, the one with the lowest elevation is selected. A point is classified

as bare earth if the maximum value of slope between this point and any other point (height difference) within a given radius (distance) is less than a predefined threshold. In practical applications, the predefined radius for the structure element is typically set to 5 m. Parameters of the filter function were determined based on the maximum terrain slope found in the area and from the height precision of the laser points [6].

D. Reference Data for Validation

There are two basic errors in filtering LiDAR data. The first one is to classify nonground measurements as ground points (Type II error), and the second one (Type I error) is to select ground points as nonground measurements [29]. Since all filtering methods are subject to these two errors, results should be examined. The validation of the point classification with the whole-point cloud is impractical due to the large number of measurements recorded. An alternative approach proposed by Zhang and Whitman [30] and Zhang *et al.* [25] that examines a sample of randomly selected test points was selected. First, a set of 50 x- and y-coordinates was selected randomly within the bounds of the T1 and T2 test sites. The sampling protocol ensured that these locations covered the terrain and vegetation variability of the study area (Fig. 1). Then, LiDAR measurements that fell within 3 m of distance to the x- and y-coordinates were selected as test points. Finally, the 424 test points selected were classified manually using a high spatial resolution ortophotography provided by the PNOA mission, the intensity image created from the LiDAR data, as well as the 3-D visualization of the points. In the case of points with higher difficulty to be classified, a field campaign was conducted. They were staked out in field using a Leica VIVA GS15 CS10 GNSS real-time kinematic (RTK) global positioning system to confirm the manual filtering and to be as precise as possible.

E. Validation

The evaluation approach used by Sithole and Vosselman [29] is adopted here to assess quantitatively and qualitatively the performance of the seven filtering methods applied. Sithole and Vosselman [29] proposed three accuracy metrics to quantitatively analyze the performance of a filter: 1) Type I error—rejection of bare-earth points (2); Type II error—acceptance of object points as bare earth (3); and total error (4)

$$Type\ I_{Error} = \frac{a}{BE} \tag{2}$$

$$Type\ II_{Error} = \frac{b}{OBJ} \tag{3}$$

$$Total_{Error} = \frac{a+b}{BE+OBJ} \tag{4}$$

where a is the number of ground points incorrectly identified as object, b is the number of object points incorrectly identified as ground, and BE and OBJ are the total number of bare earth and object points in the reference data, respectively. The total error rate is equal to the sum of all wrong classifications divided by the total number of points in the dataset [37]. Alternatively,

TABLE IV
QUALITATIVE COMPARISON OF FILTERS

Assessed objects	Filters				
	MCC	LAS tools	BCAL	ALDPAT	FUSION
Discontinuity					
Preservation (steep slopes)	***	***	*	*	**
Sharp edges (roads, terracing)	***	***	**	**	**
Small reliefs	***	***	*	*	**
Vegetation					
Vegetation	***	***	***	**	***
Vegetation on slopes	**	**	**	**	**
Low vegetation	**	**	**	**	**

*Poor (item not filtered most of the time, i.e., <50%).
**Fair (item not filtered a few times).
***Good (item filtered most of the time, i.e., >90%).

success rate was calculated as the ratio between points correctly classified and the total number of points in the dataset.

Recently published algorithms [7], [33], [37] utilize Cohen's Kappa index [58] as a measure of accuracy as this index seems to be a more robust measurement than a simple percentage [59]. This statistical coefficient measures the overall interrater agreement, accounting for the possibility of chance in the observed frequencies. Kappa index ranges generally from 0 to 1, although negative numbers are possible. According to Landis and Koch [60], values of Kappa below 0.40 present poor agreement, between 0.40 and 0.75 are considered as good agreement, and above 0.75 generally reflect excellent agreement.

Furthermore, the effect in the filtering error of four variables, such as terrain slope, land cover type, point density, and scan angle, was examined. In this sense, the error metrics were stratified based on several categories established in these variables.

Finally, the qualitative assessment of all filter procedures consists of a visual examination and comparison of a shaded relief of the DEMs developed with the filtered datasets.

III. RESULTS

A. Qualitative Assessment

The results of the qualitative assessment of filters performed following the same criteria proposed by Sithole and Vosselman [29] are summarized in Table IV. Figs. 3 and 4 exemplify miscellaneous difficulties in filtering in two samples representative of the study area. First, Fig. 3 corresponds to a complex mixture of Aleppo pine forest on a steep slope (i), pine terrace plantations (ii), and shrub vegetation about 2 m height (iii). Second, Fig. 4 consists of the area affected by fire in 2008 where a high number of bare-earth points exist (i), low vegetation on slope (ii), and pine forest (iii). The visualizations of the filtered shaded reliefs exhibit nearly the same appearance in all the samples, i.e., most of nonground object points were removed by the five filters. However, several Type I and Type II errors were committed by the filters.
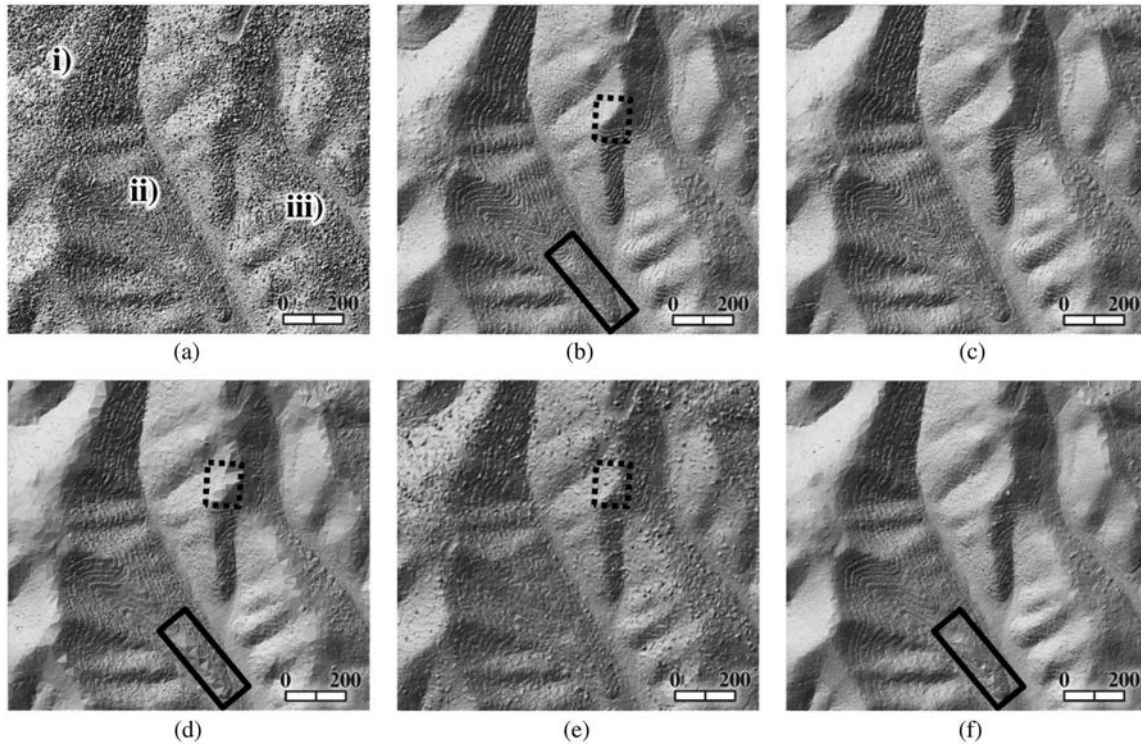
Fig. 3. 3-D surface models generated from the (a) unfiltered data and the filtered bare-earth points using (b) MCC, (c) LAStools, (d) BCAL, (e) ALDPAT-PM, and (f) FUSION filtering methods. The sampling area is characterized by (i) Aleppo pine forests on a steep slope, (ii) pine terrace plantations, and (iii) shrub vegetation about 2-m height.
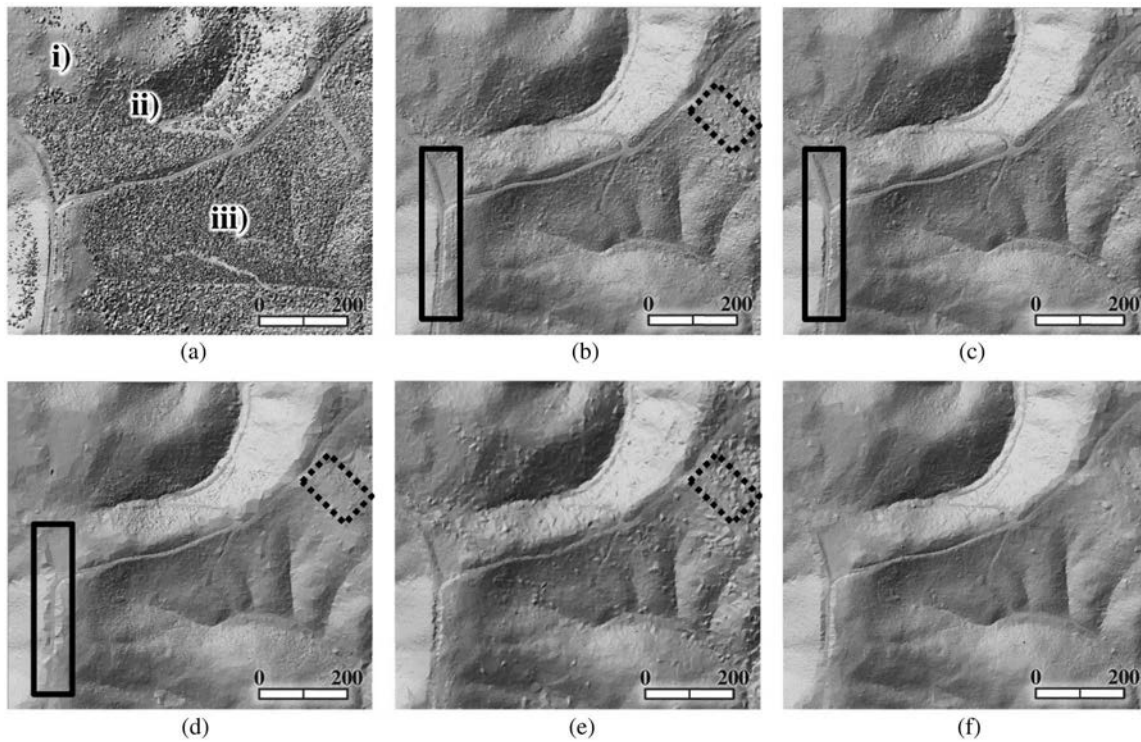

Fig. 4. 3-D surface models generated from the (a) unfiltered data and the filtered bare-earth points using: (b) MCC, (c) LAStools, (d) BCAL, (e) ALDPAT-PM, and (f) FUSION filtering methods. The sampling area is characteristic of an area affected by (i) fire in 2008, (ii) low vegetation on slope, and (iii) pine forest.

For example, a small mound (dashed line rectangle in Fig. 3) was removed completely by the BCAL filter [Fig. 3(d)] or partially contaminated by the shrub returns in ALDPAT-PM filter [Fig. 3(e)], since vegetation points were mistakenly classified as ground points. On the other hand, when the bare earth is piecewise continuous, some filters will operate as they would

TABLE V
TYPE I AND TYPE II ERRORS, SUCCESS RATE, AND COHEN'S KAPPA INDEX (p-value ≤ 0.05) OF DIFFERENT FILTERING METHODS

Filtering method	Optimum parameters	Type I error (%)	Type II error (%)	Success rate (%)	Kappa index
MCC	Scale 1, curvature 0.3	12.7	20.8	83.3	0.67
LAStools	Terrain type forest and hills, granularity fine	20.8	13.7	82.8	0.66
BCAL	All return number, canopy spacing 5, threshold value 0, inverse distance-first order interpolation method, maximum iteration 15	38.2	7.5	77.1	0.54
ALDPAT-PM	Initial cell size 1, window size 3, slope 1.2, initial threshold 0.20	39.6	14.6	72.9	0.46
FUSION	g–2.5, w 2, a 1, b 4, cell size 2	61.3	2.8	67.9	0.36
ALDPAT-ETEW	Initial cell size 1, slope 1, number of iteration 5	35.8	31.6	66.3	0.33
ALDPAT-MLS	Cell size 1, search radius 15, slope threshold 0.3	75.0	0.0	62.5	0.25

Only the results of the best settings are shown for each type of filter along with the parameters implemented.

on objects, i.e., Type I errors [29]. This is precisely what is observed in continuous line rectangles in Fig. 3(d) and (f), compared to the continuous line rectangle in Fig. 3(b), where discontinuities in the bare earth are lost, i.e., the pine terrace plantations are moderately preserved.

The roughness along the slope, denoted by the dashed line rectangles in Fig. 4(b) and (e), is created by scattered Type II errors in very low objects, i.e., presence of shrub vegetation dominated by *Quercus coccifera*. Compared to the dashed line rectangle in Fig. 4(d), the surface is generally smoother due to the high percentage of Type I errors committed by the BCAL method, as ground points were classified as nonground ones.

Finally, MCC and LAStools preserved quite well the limits of roads and forest tracks [see continuous line rectangles in Fig. 4(b) and (c)], but the rest of filtering methods present certain problems with these features. For example, the sharp edge of the road was removed partly by the BCAL, ALDPAT-PM, and FUSION filters. These algorithms tend to dilate the boundaries of areas with lower elevation relative to their neighbors [30], leading to a distortion of the surface because of this Type I error. An example of this "over filtering" can also be observed in Fig. 3(d).

B. Quantitative Assessment

First of all, to achieve optimal results, several combinations of filter parameters were applied. As a result, the parameter set presenting the minimum total error was chosen as the optimum following Hu *et al.* [59]. In Table V, the computed errors can be observed. Type I, Type II, and total errors ranged from 12.7% to 75.0%, from 0.0% to 31.6%, and from 16.7% to 37.5%, respectively. MCC filter presented the lowest overall error (16.7%), while ALDPAT-MLS and ALDPAT-ETEW filters achieved the highest overall error, 37.5% and 33.7, respectively. Type II error in MCC was 20.8%, in comparison with the 12.7% of Type I error. The inclination to commit Type II errors may not be a handicap for this filtering method, taking into consideration that Type II errors can be more easily handled by manual editing than Type I errors [29], [31], [59]. In this sense, the results obtained in MCC filtering indicated no severe biases in the

classification, as this method appropriately balanced Type II and Type I errors [19].

The second filter with the best percentage of success was LAStools, which differs from MCC in the distribution of errors. In this case, only a 13.7% of object points were misclassified as bare earth, while 20.8% of points were rejected as bare earth. A possible reason is that although the surface represented by the TIN is able to handle point density variations, the local ground surface is only relevant with three vertices and is expressed by a triangle that is simply a plane, being quite sensitive to noise [59].

With respect to ALDPAT-MLS method, it presented a high percentage of Type I errors, 75.0%, but it did not obtain Type II errors. This algorithm tends to discard many ground points, thus keeping a more sparse set of ground measurements to generate the surface. It should be noted that the sparseness of these points does not necessarily lead to a worse DEM interpolation [30]. Compared to the interpolated-based methods, the sensitivity to parameters is the major drawback in ALDPAT morphological-based filters [36], [59]. Nevertheless, the ALDPAT-PM filter committed fewer errors than ETEW and MLS methods.

Finally, to analyze the effects of the terrain slope, cover type, point density, and scan-angle variables on error rates, four comparative experiments, which are depicted in Figs. 5–8, were performed.

1) Terrain Slope: The influence of the terrain slope was evaluated using two categories: smooth slopes ranging from $0°$ up to $15°$, and steep slopes higher than $15°$ (Fig. 5).

Discontinuities or height differences are a key assumption to separate the bare earth from objects. Consequently, points significantly above their neighbors are assumed to belong to objects, but this assumption becomes difficult when the slope of the terrain increases [29]. Therefore, as expected, most filters had difficulties on steep slope higher than $15°$ (e.g., Fig. 3), increasing their error rates with the terrain complexity. In this sense, all analyzed filters, except ALDPAT-MLS, increased their Type I error. Even the filters with the lowest total error (20%) in slopes higher than $15°$, MCC and LAStools filters increased their error in this complex environments. Filters based on slope, such as ALDPAT-MLS may
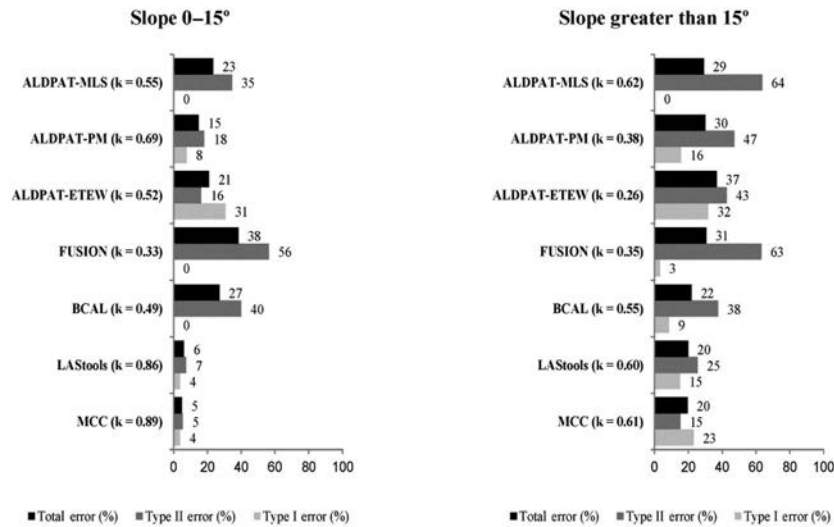
Fig. 5. Effect of terrain slope on filter performance and Cohen's Kappa index (k) (p-value ≤ 0.05).

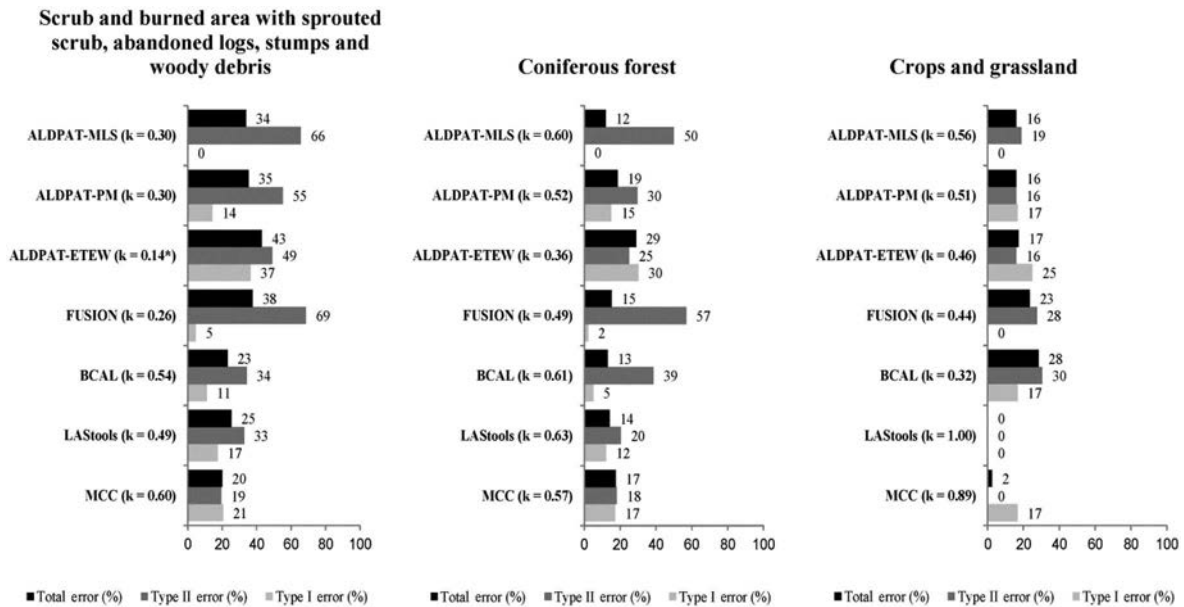Fig. 6. Effect of cover types on filter performance and Cohen's Kappa index (k) (p-value ≤ 0.05). ($*$) Nonsignificant Kappa value (p-value > 0.05).

mislabel points as nonground in areas with slopes larger than the maximum ground slope threshold. In this regard, the study area, which presents a variety of situations, from even areas to very steep ones, is challenging for ground filters because of the difficulty of selecting appropriate slope and elevation thresholds [27]. Type II errors also increased with the change in slope, mainly in the case of morphology-based filters. Furthermore, the ALDPAT filters had the highest difficulty in bare-earth discontinuities preservation, as was explained above (Fig. 3).

2) Cover Types: We also compared the performance of the algorithms within each of the main cover types of the test areas. As can be observed in Fig. 6, MCC filter was significantly better than the other six methods in terms of total error (20%) and Type II error (19%), with a good level of agreement (Kappa 0.60), particularly in scrubs and in burned areas occupied with sprouted scrub and abandoned logs. As expected, Type II errors

were higher in both types of cover due to the presence of attached and low objects such as abandoned logs, stumps, and small seedlings, as well as shrubs, which produce the classification of objects as bare earth. Points returned from shrub cover are commonly mislabeled as ground surface, as in relatively steep terrain, the slope and elevation difference between the shrub and neighboring ground points are similar to those between ground points and neighboring ground points [27].

In coniferous forest cover, ALDPAT-MLS, BCAL, and LAStools presented the best results, obtaining a low percentage of total errors, 12%, 13%, and 14%, respectively, and a good agreement. However, several tree measurements in the forest stands were classified as ground (Type II error) by many filters such as FUSION (57%) and ALDPAT-MLS (50%).

Finally, LAStools algorithm was the most suitable option in areas dominated by crops and grassland as no errors were committed.
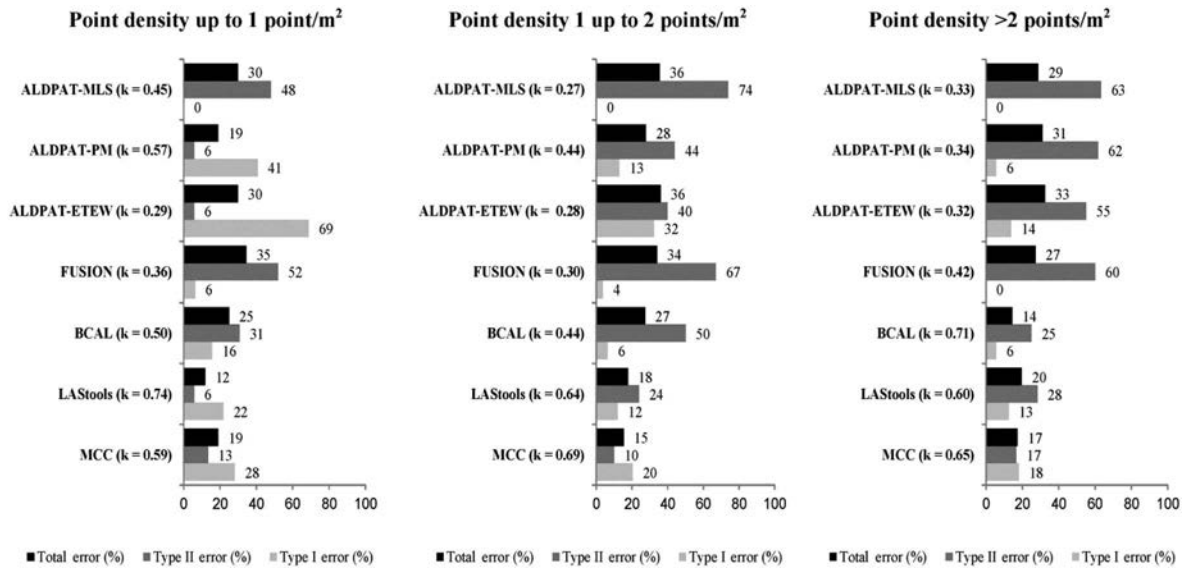
Fig. 7. Effect of point density on filter performance and Cohen's Kappa index (k) (p-value ≤ 0.05).

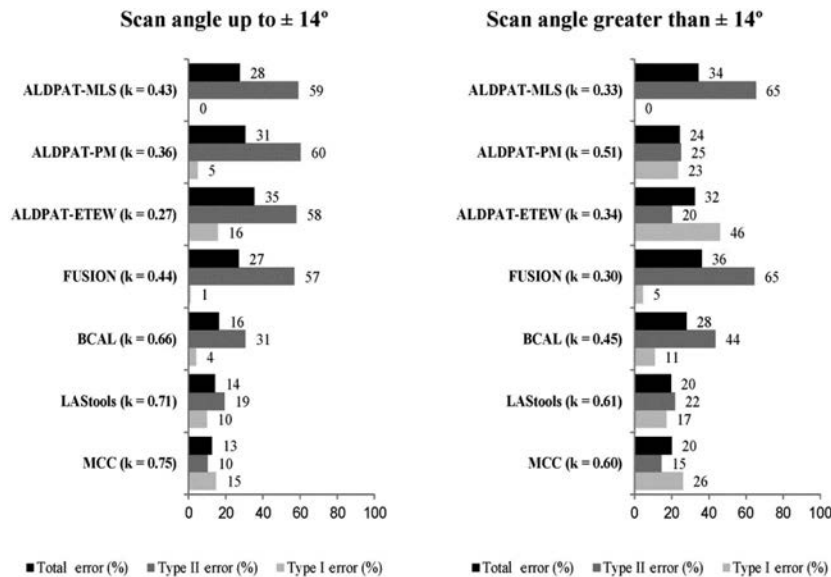Fig. 8. Effect of scan angle on filter performance and Cohen's Kappa index (k) (p-value ≤ 0.05).

3) Point Density: The effect of the variation in point density on the performance of the filter algorithms was assessed quantitatively (Fig. 7). Theoretically, if the resolution of the LiDAR data decreases, it is harder to separate the bare earth from the objects [29]. This fact results in more susceptibility to commit Type II errors on low-resolution DEMs as they are surrounded closely by ground points [30]. However, our results do not allow us to draw firm conclusions on the effect of the point density on the filter performance as also Sithole and Vosselman [29] indicated. In general, it can be seen that the Type II errors increased as did the point density, especially in the case of ALDPAT-PM (6%–62%), although BCAL, FUSION, and ALDPAT-MLS filters did not show a recognizable tendency. On the contrary, Type I errors decreased with increasing point density in all filters tested. LAStools had the lowest total error (12% with a very good Kappa index of agreement, 0.74) in areas with point

densities of $1 \text{ point}/\text{m}^2$. In short, the filters show different responses to the variations in point densities.

4) Scan Angle: Experience in the past reveled that artifacts attributed to multipathing, i.e., returns located well below the ground, often occur when scan angles exceed $12°$–$14°$, particularly in dense forest stands [61], [62]. PNOA mission is reluctant to discard those returns as the resulting return density nears the minimum specified. Therefore, the effect of scan angle on filter performance was examined. As can be seen in Fig. 8, error rates in filtering tend to increase when the scan angle is higher than $\pm 14°$. However, there are exceptions. ALDPAT-PM reduced their Total and Type II errors, but increased the Type I errors (5%–23%). This is similar in ALDPAT-ETW filter, which dramatically increased Type I error from 16% to 46%. In contrast, the rest of methods followed a different trend, increasing their error with scan angles higher than $\pm 14°$. Therefore,

it can be assumed that the ALDPAT-PM and ALDPAT-ETEW filters are less sensitive to errors introduced by the increment in scan angle, despite of their inconspicuous Kappa index. On the opposite, interpolation-based filters resulted in increased misclassifications, particularly Type I errors.

IV. DISCUSSION

LiDAR technology is recognized as a cost-effective mean of sampling the terrain surface, particularly over extensive areas, and it is increasingly becoming very important in the estimation of forest structural parameters [6].

Spain has joined the short list of countries, such as Netherlands, Belgium, Switzerland, or some parts of the United States, that have conducted national-level LiDAR programs with the purpose of providing national high-resolution DEMs (2–5 m), using this active remotely sensed data [14]. These national DEMs are typically produced by the same national agencies that collect the LiDAR data, and in those, the cost for commercial software to filter the point clouds is only marginal compared to the cost of data collection. However, this can be an issue for smaller organizations or research institutes that collect LiDAR data. This raises the question. For users who do not have access to a commercial product to filter LiDAR data, what other tools for point cloud classification are accessible?

Filtering of LiDAR point clouds into terrain and off-terrain datasets is critical in developing accurate surface models [31], [59], but the main drawback is the large number of methods developed to process the data. Several comparative reviews of some of these existing filters report strengths and weaknesses of each one [27], [29]. However, no comprehensive comparative review of nonproprietary tools (e.g., [44] and [45]) and available filtering software has been made to guide potential users of PNOA-LiDAR data in selecting a proper method.

This study tried to assess the potential of seven filtering algorithms in the classification of discrete return PNOA-LiDAR point clouds, in a Mediterranean pine forest environment. Our goal was to assist users in the selection of the best-processing method for a typical Mediterranean landscape with a variety of covers and terrain characteristics.

Ranges for the initial parameters included in the different approaches were selected by reviewing the literature of the algorithm developers, considering the study-area characteristics and comparing unfiltered and filtered results iteratively. In this sense, defining an appropriate threshold is even more important when dealing with slope-based methods [36].

In this research, the reference data used to check the filtering quality were generated by hand, classifying every point into ground and nonground ones, with the support of LiDAR-derived products, ortophotography, and fieldwork information. Optimum filters and parameters were selected through a qualitative (3-D shaded relief visualizations) and quantitative (error metrics and Kappa index) analysis of the seven algorithms. Furthermore, error associated with LiDAR classification on different landscapes and data contexts, i.e., terrain slope, land cover type, point density, and scan angle of LiDAR data, was assessed.

Our results agree with the conclusions of Sithole and Vosselman [29], who pointed out that filters are not foolproof, and the best filter algorithm and its parameters may vary from one scene condition to another. The absence of severe biases in classified ground returns (success rate of 83.3% with a Kappa index of 0.67) suggests that MCC appropriately balanced Type II and Type I errors [19]. The MCC algorithm, designed for forest landscapes, performs exceptionally well with regard to Type I errors (see Table V), thus maximizing the number of classified ground returns and increasing the detail in the bare-earth surface. For instance, footpaths and roads [Fig. 4(b)] tend to be retained very well [19]. However, in future, the research should address Type II errors, as it mistakenly classifies objects as ground, thus creating bulges and other artifacts [37]. In addition, processing time is a current drawback in the implementation of the MCC method [19].

The MCC and LAStools algorithms were successful, suggesting that novice users can achieve good results with them using minimal parameters. As Hu *et al.* [59] and Mongus and Žalik [36] noted, the sensitivity to parameters is the major downside for ALDPAT morphological-based filters, which adds value to the interpolated-based methods, such as MCC or LAStools. In fact, these two filters were the least sensitive to the presence of points on slopes higher than 15°, as indicated their total errors around 20% and the good agreement obtained (Kappa about 0.60).

ALDPAT-MLS filter, a method based on slope or height differences between neighboring points [20], was unreliable due to the large Type II errors obtained, so further investigation about the selection of a threshold to separate ground and nonground points will be needed [30]. In this method, there is still a great uncertainty about whether the differences in elevation of points are caused by the presence of objects or by variations in the terrain altitudes, especially on abrupt surfaces [28].

The results of the ALDPAT morphology-based filters showed in Table V agree with those obtained by Zhang and Whitman [30], who concluded that the PM filter produced the least error among the three methods. A common weakness of morphological methods, apart from the significant loss of information associated with the conversion of the point cloud into a raster image to perform morphological operations [36], is the difficulty in maintenance of terrain features when the window sizes are changed with the operations of openings and closings [25], [26], [28], [31]. The selection of window sizes is critical to remove suitably objects with different sizes [27], which implies using additional knowledge about the extent of objects in the study area [25], [30]. This fact prevents morphological methods from being fully automated [29], [40], [63].

In accordance with Kraus and Pfeifer [5], poor results were achieved with the linear-prediction-based method implemented in FUSION, since it uses a rough surface approximation for determining a buffer zone within which points are classified as bare earth, not preserving terrain details and misclassifying small objects [40]. The major difficulty in this method relies on the selection of customizable parameters to define the intermediate surface and a suitable threshold to classify points [36].

Vegetation density largely determines the ratio of ground to vegetation returns [19]. MCC filter performed the best with low vegetation conditions, whereas the ALDPAT-MLS and BCAL methods were somewhat more suitable for filtering the Aleppo pine forest in terms of total error, although the ALDPAT-MLS filter showed a 50% of Type II error. As Tinkham *et al.* [44] noted in their comparative study between MCC, BCAL, and another custom filter, BCAL is able to create a more reliable surface in very dense, continuous vegetation like those areas of the *Pinus halepensis* Mill. forest included in the study sites. This is most likely due to the block minimum approach that BCAL uses, allowing the creation of a surface from fewer points than MCC. On the other hand, LAStools was the only filter not committing misclassification in areas covered by crops and grasslands. In this way, users might consider the possibility of combining multiple classification procedures to exploit the strengths of each, depending on the cover type. Thus, our research supports the idea of Sithole and Vosselman [29], who suggested testing the environment to be filtered to avoid unpredictable results.

Empirical analysis regarding the selection of filter parameters in forest studies is necessary to determine which are optimal [44], but also more comparative studies focusing on open-source point classification algorithms, which are more accessible. In addition, future research should conduct a more thorough accuracy analysis in areas of higher complexity, as those occupied by low vegetation, to provide a clearer guidance to specific users [27]. In this sense, the new generation of airborne laser scanning sensors, the so-called full-waveform scanners, offer further information about the targets included in the footprint than location alone: peak amplitude which relates to radiometric properties of the target, and pulse width, which is a measure of surface roughness and slope. This additional information might be very useful to discriminate low vegetation from bare-earth reflections and might help to diminish the problems of discrete airborne LiDAR systems prior to DEM generation [64].

Additionally, filter developers are encouraged to provide more detailed information about filtering processes and parameterizations to facilitate the LiDAR data management [59].

As Sithole and Vosselman [29] pointed out, the effects of the reduced point density are most likely minor compared to the errors introduced by the complexity of the scene, such as low vegetation on steep slopes. Zhang and Whitman [30] concluded that point density has relatively less effect on the filtering results. Our results demonstrate that most of the filters can well identify bare-earth points despite the low count of bare-earth points. The complexity of the test sites determined that even at the highest resolutions, i.e., higher than 2 points/m^2, the filters encounter difficulties, which then masks the performance of the filters at lower resolutions [29]. Thus, the results showed that point densities up to 1 point/m^2 did not necessarily cause lower accuracies in the filtering process. It should be noted that the effect of point density on filter performance is also influenced by vegetation types (crops and grassland, scrubs, or forest). The point density is not only determined by the amount of emitted laser pulses but also by the presence or absence of vegetation. In forest areas, the interaction of laser pulses with tree crowns, branches, and leaves is higher, increasing the point density available for filtering and the complexity of the data.

In the case of the scanning angle, it has been shown that the error in the filtering process increases with scan angle in the progressive TIN densification and in the interpolation-based filters, which had good Kappa index of agreement. However, the morphological filters do not show this tendency.

In order to complement the results presented in this study, it would be useful to focus future research on the analysis of the error distribution in DEM generation, as this error can be propagated subsequently into derived products [16], [30]. As shown in Figs. 3 and 4, a ridge or a hilltop that is locally higher than other portions of the ground surface may resemble an above-ground object and be classified as such [31], or terrain points in steep slopes may be classified as vegetation as lie at the same height, increasing Type II errors. This poses a challenge to the surface-based filters used in this study [31]. The preservation of discontinuous ground features such as pine terrace plantations, frequent in the Mediterranean landscapes, should be better examined. In this sense, Mongus and Žalik [36] argue that preserving ridges may sometimes be unsuccessful when the surface model is created, because the interpolation procedures tend to estimate smooth terrain.

In conclusion, although most of the technical hardware difficulties have been solved, the development of more accurate algorithms and methods for modeling of LiDAR data is still necessary [31].

V. CONCLUSION

This paper proposes a comparison of seven filtering methods, implemented in nonproprietary tools and openly available software, for bare-earth extraction from PNOA-LiDAR data in a Mediterranean forest landscape. These methods, designed for filtering discrete return data, include the progressive TIN densification (LAStools), the weighted linear least-squares interpolation-based (FUSION), the multiscale curvature classification (MCC), the interpolation-based (BCAL), the elevation threshold with expand window (ALDPAT-ETEW), the progressive morphological (ALDPAT-PM), and the maximum local slope (ALDPAT-MLS) filters. As confirmed our results, a high level of accuracy is achieved by the MCC algorithm (83.3% of success rate and Kappa index of 0.67), as well as by the LAStools (82.8% of success rate and Kappa index of 0.66), compared with the rest of filtering algorithms tested. However, each method has its strengths and weaknesses as none of them worked perfectly, and all methods were susceptible to both Type I and Type II errors, due to the complexity of the earth surface, i.e., terrain slopes and cover types, and the point density and scan angle, to a lesser extent. MCC and LAStools filters produced good results, but they differed in Type I/Type II error counting. Sprouted scrub, stumps, and woody debris were the more problematic cover type in filtering, as well as terrain slopes higher than 15°. However, less firm conclusions can be drawn from point density and scan angle variables, because morphological methods are less sensitive to these factors. The quality of the LiDAR-derived DEMs directly affects the quality of the LiDAR-derived canopy heights used in subsequent

vegetation modeling, where the removal of nonground points from the raw data is a critical stage. Filtering parameters implemented in this study and the results obtained establish the first baseline for potential users of medium–low density point clouds as the PNOA-LiDAR mission, in the absence, until now, of information describing in detail the suitability of parameters and filtering methods in areas occupied by Aleppo pine forest mixed with evergreen shrub.

REFERENCES

[1] E. J. Huising and L. M. Gomes Pereira, "Errors and accuracy estimates of laser data acquired by various laser scanning systems for topographic applications," *ISPRS J. Photogramm. Remote Sens.*, vol. 53, no. 5, pp. 245–261, 1998.

[2] M. S. Renslow, *Manual of Airborne Topographic LiDAR*. Bethesda, MD, USA: ASPRS, 2012.

[3] E. P. Baltsavias, "A comparison between photogrammetry and laser scanning," *ISPRS J. Photogramm. Remote Sens.*, vol. 54, nos. 2–3, pp. 83–94, 1999.

[4] K. A. Razak, M. W. Straatsmaa, C. J. van Westen, J.-P. Malet, and S. M. de Jong, "Airborne laser scanning of forested landslides characterization: Terrain model quality and visualization," *Geomorphology*, vol. 126, pp. 186–200, 2011.

[5] K. Kraus and N. Pfeifer, "Determination of terrain models in wooded areas with airborne laser scanner data," *ISPRS J. Photogramm. Remote Sens.*, vol. 53, no. 4, pp. 193–203, 1998.

[6] G. Vosselman and H. G. Maas, *Airborne and Terrestrial Laser Scanning*. Dunbeath, Scotland: Whittles, 2010.

[7] C. Chen, Y. Li, W. Li, and H. Dai, "A multiresolution hierarchical classification algorithm for filtering airborne LiDAR data," *ISPRS J. Photogramm. Remote Sens.*, vol. 83, pp. 1–9, 2013.

[8] E. Ahokas, H. Kaartinen, and J. Hyyppä, "A quality assessment of airborne laser scanner data," *Int. Arch. Photogramm. Remote Sens. Spat. Inf. Sci.*, vol. 34, Part 3, p. W13, 2003.

[9] C. Hopkinson, "The influence of flying altitude, beam divergence, and pulse repetition frequency on laser pulse return intensity and canopy frequency distribution," *Can. J. Remote Sens.*, vol. 33, no. 4, pp. 312–324, 2007.

[10] M. E. Hodgson *et al.*, "An evaluation of LiDAR-derived elevation and terrain slope in leaf-off conditions," *Photogramm. Eng. Remote Sens.*, vol. 71, no. 7, pp. 817–823, 2005.

[11] J. Su and E. Bork, "Influence of vegetation, slope, and LiDAR sampling angle on DEM accuracy," *Photogramm. Eng. Remote Sens.*, vol. 72, no. 11, pp. 1265–1274, 2006.

[12] C. W. Bater and N. C. Coops, "Evaluating error associated with LiDAR-derived DEM interpolation," *Comput. Geosci.*, vol. 35, no. 2, pp. 289–300, 2009.

[13] J. P. Wilson, "Digital terrain modeling," *Geomorphology*, vol. 137, pp. 107–121, 2012.

[14] C. Véga, S. Durrieu, J. Morel, and T. Allouis, "A sequential iterative dual-filter for LiDAR terrain modeling optimized for complex forested environments," *Comput. Geosci.*, vol. 44, pp. 31–41, 2012.

[15] P. F. Fisher and N. J. Tate, "Causes and consequences of error in digital elevation models," *Prog. Phys. Geogr.*, vol. 30, no. 4, pp. 467–489, 2006.

[16] C. Hutton and R. Brazier, "Quantifying riparian zone structure from airborne LiDAR: Vegetation filtering, anisotropic interpolation, and uncertainty propagation," *J. Hydrol.*, vols. 442–443, pp. 36–45, 2012.

[17] G. Sohn and I. Dowman, "Terrain surface reconstruction by the use of tetrahedron model with the MDL criterion," *Int. Arch. Photogramm. Remote Sens. Spat. Inf. Sci.*, vol. 34, Part 3A, pp. 336–344, 2002.

[18] A. Kobler, N. Pfeifer, P. Ogrinc, L. Todorovski, K. Ostir, and S. Dzeroski, "Repetitive interpolation: A robust algorithm for DTM generation from aerial laser scanner data in forested terrain," *Remote Sens. Environ.*, vol. 108, no. 1, pp. 9–23, 2007.

[19] J. S. Evans and A. T. Hudak, "A multiscale curvature algorithm for classifying discrete return LiDAR in forested environments," *IEEE Trans. Geosci. Remote Sens.*, vol. 45, no. 4, pp. 1029–1038, Apr. 2007.

[20] G. Vosselman, "Slope based filtering of laser altimetry data," *Int. Arch. Photogramm. Remote Sens. Spat. Inf. Sci.*, vol. 33, Part B3, pp. 935–942, 2000.

[21] S. Filin and N. Pfeifer, "Segmentation of airborne laser scanning data using a slope adaptive neighbourhood," *ISPRS J. Photogramm. Remote Sens.*, vol. 60, no. 2, pp. 71–80, 2006.

[22] C. K. Wang and Y. H. Tseng, "DEM generation from airborne LiDAR data by an adaptive dual-directional slope filter," *Int. Arch. Photogramm. Remote Sens. Spat. Inf. Sci.*, vol. 38, Part 7B, pp. 628–632, 2010.

[23] D. Tóvári and N. Pfeifer, "Segmentation based robust interpolation—A new approach to laser data filtering," in *Proc. ISPRS Workshop Laser Scann. (WG III/3, III/4, V/3)*, Enschede, The Netherlands, 2005, 6 pp.

[24] J. Kilian, N. Haala, and M. Englich, "Capture and evaluation of airborne laser scanner data," *Int. Arch. Photogramm. Remote Sens.*, vol. 31, Part B3, pp. 383–388, 1996.

[25] K. Zhang, S. C. Chen, D. Whitman, M. L. Shyu, J. Yan, and C. Zhang, "A progressive morphological filter for removing non ground measurements from airborne LiDAR data," *IEEE Trans. Geosci. Remote Sens.*, vol. 41, no. 4, pp. 872–82, Apr. 2003.

[26] Q. Chen, P. Gong, D. Baldocchi, and G. Xie, "Filtering airborne laser scanning data with morphological methods," *Photogramm. Eng. Remote Sens.*, vol. 73, no. 2, pp. 175–185, 2007.

[27] X. Meng, N. Currit, and K. Zhao, "Ground filtering algorithms for airborne LiDAR data: A review of critical issues," *Remote Sens.*, vol. 2, no. 3, pp. 833–860, 2010.

[28] Y. Li, H. Wu, H. Xu, R. An, J. Xu, and Q. He, "A gradient-constrained morphological filtering algorithm for airborne LiDAR," *Opt. Laser Technol.*, vol. 54, pp. 288–296, 2013.

[29] G. Sithole and G. Vosselman, "Experimental comparison of filter algorithms for bare-earth extraction from airborne laser scanning point clouds," *ISPRS J. Photogramm. Remote Sens*, vol. 59, nos. 1–2, pp. 85–101, 2004.

[30] K. Zhang and D. Whitman, "Comparison of three algorithms for filtering airborne LiDAR data," *Photogramm. Eng. Remote Sens.*, vol. 71, no. 3, pp. 313–324, 2005.

[31] J. Zhang and X. Lin, "Filtering airborne LiDAR data by embedding smoothness-constrained segmentation in progressive TIN densification," *ISPRS J. Photogramm. Remote Sens.*, vol. 81, pp. 44–59, 2013.

[32] P. Axelsson, "DEM generation from laser scanner data using adaptive TIN models," *Int. Arch. Photogramm. Remote Sens.*, vol. 33, Part B4/1, pp. 110–117, 2000.

[33] J. L. Silván-Cárdenas and L. Wang, "A multi-resolution approach for filtering LiDAR altimetry data," *ISPRS J. Photogramm. Remote Sens.*, vol. 61, no. 1, pp. 11–22, 2006.

[34] G. Y. Lu and D. W. Wong, "An adaptive inverse-distance weighting spatial interpolation technique," *Comput. Geosci.*, vol. 34, no. 9, pp. 1044–1055, 2008.

[35] X. Meng, L. Wang, J. L. Silván-Cárdenas, and N. Currit, "A multi-directional ground filtering algorithm for airborne LiDAR," *ISPRS J. Photogramm. Remote Sens.*, vol. 64, no. 1, pp. 117–124, 2009.

[36] D. Mongus and B. Žalik, "Parameter-freeground filtering of LiDAR data for automatic DTM generation," *ISPRS J. Photogramm. Remote Sens.*, vol. 67, pp. 1–12, 2012.

[37] T. J. Pingel, K. C. Clarke, and W. A. McBride, "An improved simple morphological filter for the terrain classification of airborne LiDAR data," *ISPRS J. Photogramm. Remote Sens.*, vol. 77, pp. 21–30, 2013.

[38] C. Brenner, "Towards fully automatic generation of city models. International archives of the photogrammetry," *Remote Sens. Spat. Inf. Sci.*, vol. 33, Part 3B, pp. 85–92, 2000.

[39] W. Zhou and A. Troy, "An object-oriented approach for analysing and characterizing urban landscape at the parcel level," *Int. J. Remote Sens.*, vol. 29, Part 11, pp. 3119–3135, 2008.

[40] M. Bartels and H. Wei, "Threshold-free object and ground point separation in LiDAR data," *Pattern Recognit. Lett.*, vol. 31, no. 10, pp. 1089–1099, 2010.

[41] M. Bartels and H. Wei, "Segmentation of LiDAR data using measures of distribution," *Int. Arch. Photogramm. Remote Sens. Spat. Inf. Sci.*, vol. 36, Part 7, pp. 426–431, 2006.

[42] Y. Bao *et al.*, "Classification of LiDAR point cloud and generation of DTM from LiDAR height and intensity data in forested area," *Int. Arch. Photogramm. Remote Sens. Spat. Inf. Sci.*, vol. 37, Part 3B, pp. 313–318, 2008.

[43] A. B. Jahromi, M. J. V. Zoej, A. Mohammadzadeh, and S. Sadeghian, "A novel filtering algorithm for bare-earth extraction from airborne laser scanning data using an artificial neural network," *IEEE J. Sel. Topics Appl. Earth Observ. Remote Sens.*, vol. 4, no. 4, pp. 836–843, Dec. 2011.

[44] W. T. Tinkham *et al.*, "A comparison of two open source LiDAR surface classification algorithms," *Remote Sens.*, vol. 3, pp. 638–649, 2011.

[45] K. Korzeniowska, N. Pfeifer, G. Mandlburger, and A. Lugmayr, "Experimental evaluation of ALS point cloud ground extraction tools over different terrain slope and land-cover types," *Int. J. Remote Sens.*, vol. 35, pp. 4673–4697, 2014.

[46] S. M. Vicente-Serrano, T. Lasanta, and C. Gracia, "Aridification determines changes in forest growth in Pinus halepensis forests under semiarid Mediterranean climate conditions," *Agric. For. Meteorol.*, vol. 150, no. 4, pp. 614–628, 2010.

[47] E. Notivol, A. Cabanillas, R. González, and C. Revuelta, "Caracterización de masas naturales de pino carrasco (Pinus halepensis Mill.) en la Depresión del Ebro," in *Proc. 4° Congreso Forestal Español La ciencia Forestal: Respuestas para la Sostenibilidad*, 2005, 7 pp.

[48] M. Tanase, J. de la Riva, and F. Pérez-Cabello, "Estimating burn severity at the regional level using optically based indices," *Can. J. For. Res.*, vol. 41, no. 4, pp. 863–872, 2011.

[49] M. Tanase, J. de la Riva, M. Santoro, F. Pérez-Cabello, and E. Kasischke, "Sensitivity of SAR data to post-fire forest regrowth in mediterranean and boreal forests," *Remote Sens. Environ.*, vol. 115, pp. 2075–2085, 2011.

[50] E. Chuvieco, *Earth Observation of Wildland Fires in Mediterranean Ecosystems*. Berlin, Germany: Springer-Verlag, 2009, 257 pp.

[51] P. Axelsson, "Processing of laser scanner data—Algorithms and applications," *ISPRS J. Photogramm. Remote Sens.*, vol. 54, nos. 2–3, pp. 138–147, 1999.

[52] R. McGaughey, *FUSION/LDV: Software for LIDAR Data Analysis and Visualization*. Seattle, WA, USA: US Dept. Agriculture, Forest Service, Pacific Northwest Research Station, 2009, 175 pp.

[53] K. Kraus and E. Mikhail, "Linear least squares interpolation," *Photogramm. Eng.*, vol. 38, pp. 1016–1029, 1972.

[54] A. S. Maguya, V. Junttila, and T. Kauranne, "Adaptive algorithm for large scale DTM interpolation from LiDAR data for forestry applications in steep forested terrain," *ISPRS J. Photogramm. Remote Sens.*, vol. 85, pp. 74–83, 2013.

[55] D. Streutker and N. Glenn, "LiDAR measurement of sagebrush steppe vegetation heights," *Remote Sens. Environ.*, vol. 102, nos. 1–2, pp. 135–145, 2006.

[56] K. Zhang and Z. Cui, *Airborne LIDAR Data Processing and Analysis Tools. ALDPAT 1.0*. Miami, FL, USA: National Center for Airborne Laser Mapping, 2007, 81 pp.

[57] P. Soille, *Morphological image analysis: Principles and applications*. New York, NY, USA: Springer, 2003, 392 pp.

[58] J. Cohen, "A coefficient of agreement for nominal scales," *Educ. Psychol. Meas.*, vol. 20, pp. 37–46, 1960.

[59] H. Hu *et al.*, "An adaptive surface filter for airborne laser scanning point clouds by means of regularization and bending energy," *ISPRS J. Photogramm. Remote Sens.*, vol. 92, pp. 98–111, 2014.

[60] J. R. Landis and G. G. Koch, "The measurement of observer agreement for categorical data," *Biometrics*, vol. 33, pp. 159–174, 1977.

[61] D. Gatziolis and H. E. Andersen, "A guide to LiDAR data acquisition and processing for the forests of the Pacific Northwest," US Dept. Agriculture, Forest Service, Pacific Northwest Research Station, Portland, OR, USA, General Tech. Rep. PNW-GTR-768, 2008, 32 pp.

[62] J. Holmgren and M. Nilsson, "Simulating the effects of LiDAR scanning angle for estimation of mean tree height and canopy closure," *Can. J. Remote Sens.*, vol. 29, no. 5, pp. 623–632, 2003.

[63] X. Liu, "Airborne LiDAR for DEM generation: Some critical issues," *Prog. Phys. Geogr.*, vol. 32, no. 1, pp. 31–49, 2008.

[64] G. Vosselman and H. G. Maas, *Airborne and Terrestrial Laser Scanning*. Dunbeath, Scotland: Whittles, 2010.

Antonio Luis Montealegre was born in Barcelona, Spain, in 1986. He received the Bachelor's degree in geography and the Master's degree in geographic information technologies for land management: geographic information systems (GIS) and remote sensing from the University of Zaragoza, Zaragoza, Spain, in 2009 and 2010, respectively. He is currently pursuing the Ph.D. degree in geography and land management at the same university.

Since March 2011, his work has been financed by the Government of Aragón, Department of Science, Technology and University, being involved in the activities of the GEOFOREST Research Group, Environmental Sciences Institute, University of Zaragoza. His research interests include LiDAR remote sensing data processing techniques, applied particularly to fire severity assessment, forest inventory, fuel type modeling, and DEMs generation.

María Teresa Lamelas was born in Zaragoza, Spain, in 1977. She received the Ph.D. degrees in geography and in natural sciences from the University of Zaragoza, Zaragoza, Spain, and Damstadt University of Technology, Damstadt, Germany, respectively, in 2007.

From 2008 to 2012, she was an Associated Teacher with the Department of Geography and Land Management, University of Zaragoza. Since 2012, she has been teaching the subject "geographical information systems and remote sensing" and has been a Researcher in the same topic with the Centro Universitario de la Defensa in Zaragoza, Zaragoza, Spain. She is Member of the GEOFOREST Research Group, Environmental Sciences Institute, University of Zaragoza. Her research interests include the use of geographical information technologies in natural resources and hazards modeling.

Juan de la Riva received the Ph.D. degree in geography from the University of Zaragoza, Zaragoza, Spain, in 1994.

He is currently a Professor of Regional Geographic Analysis with the University of Zaragoza, where he coordinates the GIS and remote sensing master course. He is the Head of the GEOFOREST Research Group, Environmental Sciences Institute, University of Zaragoza, and has worked in different management studies in mountain areas, as well as in several research projects, namely, FIRERISK, EROFUEGO, LIGNOSTRUM, RS-FIRE, PIR-FIRE, and FIREGLOBE. His research interests include the study of forested areas, application of GIS and remote sensing techniques, use of remote sensing and GIS for forest characterization, forest fires (risk modeling, fire severity, and postfire environmental dynamic) assessment, and biomass estimation.